International Journal of Advanced Engineering Research and Science (IJAERS)
Peer-Reviewed Journal
ISSN: 2349-6495(P) | 2456-1908(O)
Vol-11, Issue-1; Jan, 2024
Journal Home Page Available: https://ijaers.com/
Article DOI: https://dx.doi.org/10.22161/ijaers.11.4

Particle Swarm Algorithm Applied to Image Reconstruction on Multiphase Flows

B. C. B. N. Souza[1], R. A. M. Junior[2], M. G. Nascimento[3], C. S. Gonçalves[4], D. V. B. Siqueira[5], R. A. Câmara[6]

[1]Departamento de Física – UFPB, UFPB Campus I, Cidade Universitária, S/N – João Pessoa, Paraíba, Brazil CEP: 58.051-900
[2]Departamento de Energias Alternativas Renováveis, CEAR – UFPB, UFPB Campus I, Cidade Universitária, S/N – João Pessoa, Paraíba, Brazil CEP: 58.051-900
[3]Departamento de Engenharia Civil e Ambiental – DECA – UFPB, UFPB Campus I, Cidade Universitária, S/N – João Pessoa, Paraíba, Brazil CEP: 58.051-900
[4]Departamento de Física – UFPB, UFPB Campus I, Cidade Universitária, S/N – João Pessoa, Paraíba, Brazil CEP: 58.051-900
[5]Departamento de Física – UFPB, UFPB Campus I, Cidade Universitária, S/N – João Pessoa, Paraíba, Brazil CEP: 58.051-900
[6]Centro de Energia Alternativa e Renováveis – CEAR – UFPB, UFPB Campus I, Cidade Universitária, S/N – João Pessoa, Paraíba, Brazil CEP: 58.051-900

Received: 29 Nov 2023,

Receive in revised form: 01 Jan 2024,

Accepted: 08 Jan 2024,

Available online: 19 Jan 2024

***Keywords*—Electrical tomography, finite elements, inverse problems, particle swarm optimization, parallel processing, multiphase systems.**

Abstract *— This work presents a methodology for reconstructing multiphase flow electrical capacitive tomography (ECT) images, using a particle swarm optimization (PSO) algorithm in the parallel processing paradigm. Intended is to improve the efficiency of the inverse problem algorithm in ECT, increasing the resolution of the reconstructed images, without necessarily increasing the processing time of these reconstruction technique. A limitation found is that, for inverse problem-type reconstruction techniques for ECT, the response of the sensor system is non-linear and, therefore, the processing time grows faster than any increase in resolution, imposing a high computational cost. For real-time applications, the first contribution is the removal of unnecessary processing from the usual code; the second is the creation of a new PSO algorithm for image reconstruction that is more efficient than normal. The new parallel processing routine present the physical principles of ECT, the heuristic algorithms used in the reconstruction process and the main concepts for parallel computing.*

I. INTRODUCTION

Multiphase flows are often present in numerous industrial processes, particularly in food, chemical and petroleum industries and also in energy plants, among others (Thorn, Johansen and Hjertaker, 2013; Zainal-Mokhtar and Mohamad-Saleh, 2013; Cui et al, 2014; Mei et al, 2016). In the majority of these studied flows the dielectric nature of matter dominates, and consequently, the use of electrical capacitance tomography (ECT) is reinforced as one of the most advantageous tomographic method to obtain images from such industrial processes. In comparison to other tomographic techniques, ECT offers some advantages, such as i) been non-radioactive, ii) non-invasive and non-intrusive, iii) cost effective, iv) non susceptible to adverse temperature and pressure conditions and v) relative fast response.

This technique is based on measurement of capacitance changes in dielectric distribution of the material present in the multiphase flow. Electrodes are placed around the flow pipe, usually 8 to 16, and the capacitance values across each pair are measured. Those capacitance measurements are then applied to an appropriate reconstruction algorithm which produces an image of the dielectric spatial

distribution and therefore the material across the sensor (Yang and Peng, 2003).

The ECT sensor is composed by a number of electrodes that can be made of a cooper sheet placed around the flow pipe in a non-parallel way. Besides the capacitive sensor, there are also i) an electronic system of transduction to read a voltage signal which is proportional to the capacitance and between each pair of electrodes, and ii) a control and acquisition system that coordinates the multi-electrode measurements and converts the analog signal into the data to be used by the image reconstruction algorithm.

II. METHOD

2.1 Forward and inverse problem of ECT

Due to its specific features, ECT is considered as a soft-field tomography. Therefore, the material to be imaged modifies the electric sensing field. Such effect is highly non-linear and the image reconstruction process becomes more complex in comparison to conventional x-ray tomography (Belo, 1999).

Image reconstruction using ECT is a two steps task: firstly, the forward problem should be solved, in other words, it is the determination, using the excitation data, of the electric potentials inside the domain and the respective response along the contour. Secondly, the inverse problem should then be solved, which is the determination of the dielectric distribution into the domain from the relation between excitation data and the boundary response.

Forward Problem Solution

The solution of the forward problem associated with ECT can be defined as the determination of the electric potential, and thus the capacitance between the electrodes, associated to a given dielectric distribution over the area of a cross section of the pipe in study.

If there are no free charges within the section of the imaged region, the relationship between the capacitance and permittivity distribution is modeled by Equation (1):

$$\vec{\nabla}\left[\varepsilon_o \varepsilon(x,y)\vec{\nabla}\varphi(x,y)\right] = 0 \quad (1)$$

where $(x,y) \in \Omega$ represents the space domain, ε_0 is the vacuum absolute permittivity, $\varepsilon(x,y)$ is the relative permittivity distribution of the material inside the imaged region, $\varphi(x,y)$ is the electric potential and Γ is the closed curve enclosing the electrodes surrounding the region.

The boundary conditions are defined when an electrode is excited with a potential $\varphi = V_0$ (source electrode) and all others are kept on ground level ($\varphi = 0$). The measuring process is then multiplexed for each grounded electrode (sensing electrode) in order to obtain the respective capacitance. Therefore, the potential distribution is expressed as

$$\varphi(x,y) = \begin{cases} V_0, (x,y) \in \Omega_i \\ 0, (x,y) \in \Omega_k, k \neq i \end{cases} \quad (2)$$

and for the capacitance we have

$$C = \frac{-\varepsilon_0}{V_c} \int_\Gamma \varepsilon(x,y)\vec{\nabla}\varphi(x,y)d\Omega \quad (3)$$

As long as there is not a general analytic solution for all configurations of permittivity distribution and electrodes excitation conditions, only particular solutions can be achieved for specific configurations. For example, numerical routines using finite element method (FEM) have been developed to determine the capacitance values from the permittivity distribution and excitation profile of electrodes surrounding a pipe (Souza, 2009).

FEM was chosen due to its versatility and robustness in dealing with complex geometries and inhomogeneous media and this is also the method implemented here to solve the forward problem.

Inverse Problem Solution

Solution of the inverse problem associated to ECT can be defined as the determination of the dielectric distribution over the area of a cross section of the pipe under analysis which is related to the capacitance values obtained by the sensor.

One method of accomplishing this is to compare estimated values obtained from a numerical model with experimental measurements from a capacitance sensor. Thus, the traditional tomography problem is moved to the minimization of an error functional. Such functional should be able to reflect the discrepancies between the experimental measurements values and numerically calculated values corresponding to changes in permittivity distribution inside the region to be imaged.

The optimization process consists in a search algorithm for the dielectric distribution that globally minimizes the error functional (Smolik, 2010). At initialization, the forward problem is solved for a given initial distribution which results in a numerical answer to the capacitance value that gives a new value to the error functional. If such value is smaller than the earlier value, then the former distribution is updated and this process will be iterated many times until a global minimum for the error functional is found. When the process ends the ultimate numerical result obtained should correspond to the distribution that most resembles to the actual permittivity distribution inside the sensor, in other words, an image of the sensor cross section is achieved.

When choosing a reconstruction algorithm, the main considerations that we should take into account are computational effort, speed and accuracy. Iterative

algorithms can increase accuracy but, on the other hand, may slow the rebuilding process. Image reconstruction process using iterative approach is time consuming, because it has to estimate the capacitance value by solving the forward problem many times, in an iterated fashion, thus becoming a low-speed reconstruction technique, one that cannot be applied to systems that require real-time images.

2.2 RECONSTRUCTION ALGORITHM

Unlike direct algorithms, the iterative algorithms are formulated in terms of an optimization problem, characterized by iterated attempts to minimize an error function between the capacitance values obtained by the theoretical solution of the forward problem and experimental capacitance values obtained by the system sensor. It is assumed as the solution of the inverse problem, the dielectric configuration that can minimize the error functional (Li, 2015).

Particle Swarm Optimization

Particle Swarm Optimization (PSO) is a stochastic computational technique based on population dynamics. PSO has emerged from experiences developed by Kennedy and Eberhart (1995) with algorithms that model a social behavior from a set of individuals.

Likewise, other collective intelligence approaches, PSO is based on the skills of a population of individuals which are able to interact with each other and also the environment. Relying on the capabilities of self-evaluation, comparison and imitation, individuals are able to deal with a number of possible situations presented by the environment and therefore, global behaviors emerge from these interactions. The algorithm developed by Kennedy and Ebehart (1995) seeks the optimization of a fitness function using information exchanges among individuals (particles) and the whole population (swarm).

In order to achieve the optimal solution, each particle in PSO is treated as a point in R^n space and it represents a potential solution of the forward problem. Particle position is adjusted according to its own experience as well as group experience. Equation (4) corresponds to the sum of three distinct terms: the first one refers to the particle inertia; the second is a cognitive term related to particle individual learning of the best position it had already reached; the third is a social term that represents the experience exchange among all particles. In each iteration, the particle position is updated according to Equation (5) which considers its current position as well as a displacement given by the velocity due to iterating process.

$$v_i = wv_i + c_1 r_1 (p_{best} - x_i) + c_2 r_2 (g_{best} - x_i) \quad (4)$$

$$x_i = x_i + v_i \quad (5)$$

Where v_i is the particle i current velocity, w is an inertial weight that balances global and local exploration, c_1 and c_2 are behavior coefficients, r_1 and r_2 are random numbers between 0 and 1, p_{best} is the best position already reached by the particle and g_{best} is the best position found by the swarm.

Velocity update of particles depends on parameters that should be adjusted for each problem to be optimized, namely the inertial weight, cognitive and social terms. Inertial weight w allows broadness on the exploration space: high values improve global exploration. To the contrary, small values favor local exploration. In this work, the inertial weight has an update procedure (Equation 6) identical to what is described in Eberhart and Shi (2001), where w is adjusted linearly in the interval 0.4 to 0.9. Shi and Eberhart (1998) suggested to keep $c_1 = c_2 = 2.0$ in order to balance social and cognitive behavior of the particle.

$$w = w_{max} - (w_{max} - w_{min}) \frac{(k-1)}{m} \quad (6)$$

Where k is the iteration number, m is the maximum iteration number, w_{max} and w_{min} are the maximum and minimum weight, respectively. The steps for implementing PSO algorithm are described in the Pseudocode 1 (Eberhart and Shi, 2001):

Pseudocode 1. PSO algorithm

```
initialize constants m, n, c1, c2, w;
randomly initialize n positions and velocities in the space R^n;
for k ← 1 to m do
    for i ← 1 to n do
        solve forward problem for position i;
        evaluate fitness f(x_i);
    end for
    for i ← 1 to n do
        if f_k^i ≤ f_p^i then
            f_p^i = f_k^i
            p_best = x_k^i
        end if
        if f_k^i ≤ f_g then
            f_g = f_k^i
            g_best = x_k^i
        end if
    end for
    update velocity according to Equation (4);
    update position according to Equation (5);
    update w according to Equation (6);
end for
```

Result: *assume g_{best} as the problem solution;*

Parallel algorithm implementation of PSO can be described as a master-slave paradigm (Schutte *et al*, 2004). The master processor (MP) creates a set of random initial positions in the space R^n, partitions this set into subsets and

sends them to have its fitness function analyzed by the slave processors (SPs). All decision processes are carried out by the MP, for instance, position and velocity update as well as the algorithm convergence control. SPs solve the forward problem and compare their results to the capacitance values obtained experimentally. Thus, for each position configuration the fitness function is evaluated and the resulting value is returned to the MP. MP and SPs tasks are described in Pseudocode 2.

Pseudocode 2. Parallel PSO algorithm

```
if my_id = 0 then                          // I am the master
    initialize constants iter_max, n, c1, c2, w;
    randomly initialize n positions and velocities in the space R^n;
end if
for k ← 1 to iter_max do
    if my_id = 0 then                      // I am the master
        for target ← 1 to n_processors do
            send position x_i of m particles to each slave
        end for
        for source ← 1 to n_processors do
            receive position x_i of m particles from each slave;
            receive fitness f(x_i) of m particles from each slave;
        end for
        perform barrier synchronization for all fitness evaluation results;
        for i ← 1 to n do
            if f_k^i ≤ f_p^i then
                f_p^i = f_k^i
                p_best = x_k^i
            end if
            if f_k^i ≤ f_g then
                f_g = f_k^i
                g_best = x_k^i
            end if
        end for
        update velocity according to Equation (4);
        update position according to Equation (5);
        update w according to Equation (6);
    else                                   // I am a slave
        receive position x_i of m particles from the master;
        for i ← 1 to m do
            solve forward problem for each x_i;
            evaluate fitness f(x_i);
        end for
        send fitness f(x_i) of m particles back to the master;
    end if
end for
```

Result: *Assume g_{best} as the problem solution;*

The initial steps of serial and parallel PSO algorithms are the same. Once the initialization step has been carried out by the MP, a package of *m* particles is sent to the SPs where the fitness function for each particle is evaluated.

Information exchange between MP and SPs is implemented using Message Passing Interface (MPI), a peer-to-peer communication library, as described in Singh (2012).

Parallel algorithm application aims to reduce processing time span from capacitance measurements (from sensor) to image reconstruction in comparison to serial algorithm. Such reduction is attained by the distribution of forward problem solving to many processors.

2.3 EVALUATION OF ALGORITHMS BY SIMULATION

Algorithm process

To analyze the spatial resolution obtained by the PSO algorithm applied to the ECT, we numerically simulated the response of a capacitive sensor with eight electrodes, with 3 different distributions of a two-phase mixture (oil-water): A core flow distribution, a homogeneous distribution of oil water containing bubbles and finally a stratified distribution.

Capacitance values were obtained from the direct problem solution for simulated values of permittivity, where they were contaminated with numerical noise in order to observe the impact of experimental error in the quality of the reconstructed image. The relative permittivity of the materials was admitted to be *4.1*, *3.0* and *80.0*, respectively for the acrylic pipe, oil and water contained within the pipe.

During the process of image reconstruction, a structured mesh was used, subdividing the region under study in two subregions – inner portion and pipe wall as can be seen in Figure 1a) and 1b). In order to avoid the "inverse crime" described in Wirgin (2004), we used a more refined mesh to compute the simulated capacitance values and a less refined mesh for the solution of the inverse problem.

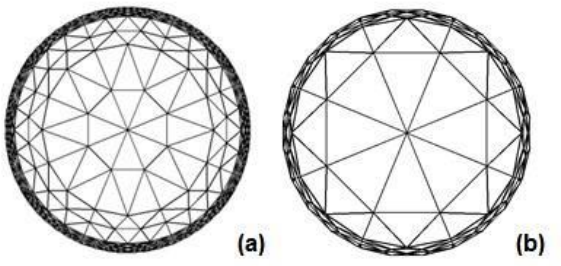

Fig.1. Discretization domain with (a) 128 elements and (b) 32 elements inside the pipe.

For the execution of the numerical routines, it was used a computer with an Intel® Core™ i7–4790, 16 GB of RAM, running Ubuntu operational system and GNU/Linux 64 bits kernel 15.10.

A cluster was assembled using a set of virtual machines on VirtualBox 4.1.8 running OpenMP protocol library.

The processing algorithm was coded in Fortran 90 language, using the GNU Fortran compiler. For pre- and post-processing, routines developed in Scilab language have been implemented.

Evaluation criteria

Two quality assessment methods were employed to evaluate the obtained images: qualitative and quantitative. The qualitative assessment involves visual comparisons of similarity for different reconstruction methods.

Reconstructed images obtained from the pipe section are also compared quantitatively using the following estimators:

a) Normalized mean square error (NMSE):

$$\Delta\varepsilon = \frac{\sum_{i=1}^{N}\left(\varepsilon_i^{\text{ref}} - \varepsilon_i^{rec}\right)^2}{\sum_{i=1}^{N}\left(\varepsilon_i^{\text{ref}} - \bar{\varepsilon}_i^{rec}\right)^2} \quad (7)$$

b) Normalized absolute error – NAE:

$$\delta\varepsilon = \frac{\sum_{i=1}^{N}\left|\varepsilon_i^{ref} - \varepsilon_i^{rec}\right|}{\sum_{i=1}^{N}\left|\bar{\varepsilon}_i^{ref}\right|} \quad (8)$$

c) Correlation coefficient – R_{xy}:

$$R_{xy} = \frac{\sum_{i=1}^{N}\left(\varepsilon_i^{rec} - \bar{\varepsilon}^{rec}\right)\left(\varepsilon_i^{\text{ref}} - \bar{\varepsilon}^{\text{ref}}\right)}{\left[\left(\sum_{i=1}^{N}\left(\varepsilon_i^{rec} - \bar{\varepsilon}^{rec}\right)^2\right)\left(\sum_{i=1}^{N}\left(\varepsilon_i^{\text{ref}} - \bar{\varepsilon}^{\text{ref}}\right)^2\right)\right]^{\frac{1}{2}}} \quad (9)$$

Where $\varepsilon_i^{\text{ref}}$ and ε_i^{rec} are respectively the permittivity value of the element i for the reference dielectric distribution and reconstruted dielectric distribution by LBP algorithm and PSO, and $\bar{\varepsilon}^{\text{ref}}$ and $\bar{\varepsilon}^{\text{rec}}$ are their average values, respectively.

The best algorithm is the one with small values of $\delta\varepsilon$ and $\Delta\varepsilon$, and values of R_{xy} close to unity. The normalized quadratic error is sensitive to large errors of some elements, while the normalized absolute error is sensitive to small errors on many factors, where the correlation coefficient indicates the spatial similarity between the reference image and the reconstructed image.

III. RESULTS

Images of the simulated flows profiles are shown on Figure 2. Those images should be compared with Figures 3, 4 and 5 for the qualitative evaluation of the results. Numerical noise of 3% and 5% were also added to the capacitance values in order to test the robustness of reconstruction algorithms.

In order to compare the quality of images obtained by the PSO algorithm, we employed linear back projection (LBP) algorithm as reference for the simulated flows shown on Figure 2. Based on the sensitivity matrix model, LBP is still the most cited reconstruction method and in its simplest implementation it presumes that the sensitivity matrix is invariant within the studied area (Li, 2015). All images were accomplished using a 5000 particles swarm and 500 iterations.

Numerical evaluation for the chosen estimators is listed on Tables 1, 2 and 3 for capacitance values without numerical noise, 3% and 5% of noise, respectively.

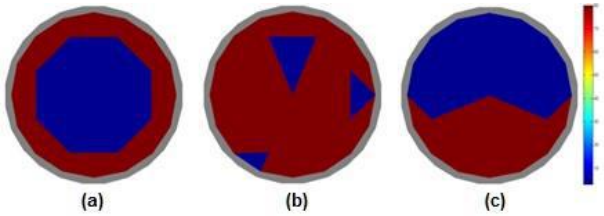

Fig.2. Dielectric simulated flow profiles: (a) core flow, (b) bubbles and (c) stratified.

Table 1. Error values ε related to the image reconstruction process without numerical noise.

Flow Pattern	Method	NMSE (%)	NAE (%)	R_{xy}
CORE	LBP	57.901	56.971	92.967
	PSO	0.137	0.112	99.999
BUBBLE	LBP	103.510	125.670	22.890
	PSO	0.010	0.010	100.000
STRATIFIED	LBP	51.758	32.230	85.891
	PSO	2.842	1.883	99.961

Table 2. Error values ε related to the image reconstruction process with numerical noise of 3%.

Flow Pattern	Method	NMSE (%)	NAE (%)	R_{xy}
CORE	LBP	59.134	58.560	91.836
	PSO	9.831	4.472	99.548
BUBBLE	LBP	102.462	123.595	22.653
	PSO	36.812	24.552	93.523
STRATIFIED	LBP	51.189	31.665	86.197
	PSO	6.281	3.400	99.815

Table 3. Error values ε related to the image reconstruction process with numerical noise of 5%.

Flow Pattern	Method	NMSE (%)	NAE (%)	R_{xy}
CORE	LBP	62.440	64.772	90.778
	PSO	18.389	7.613	98.400
BUBBLE	LBP	102.998	122.218	21.327
	PSO	55.840	37.547	85.370
STRATIFIED	LBP	52.236	33.208	85.652
	PSO	9.856	5.542	99.547

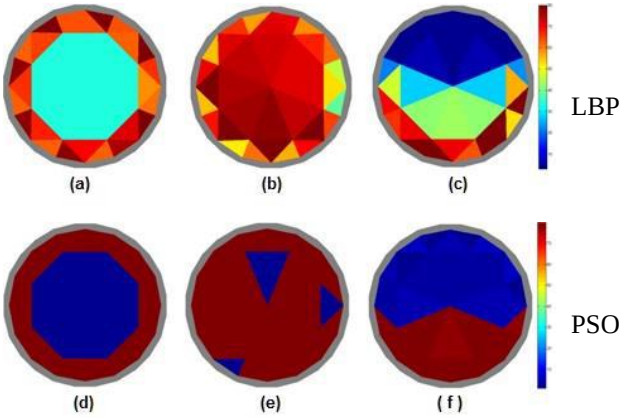

Figure 3. Reconstructed images from simulated values without numerical noise.

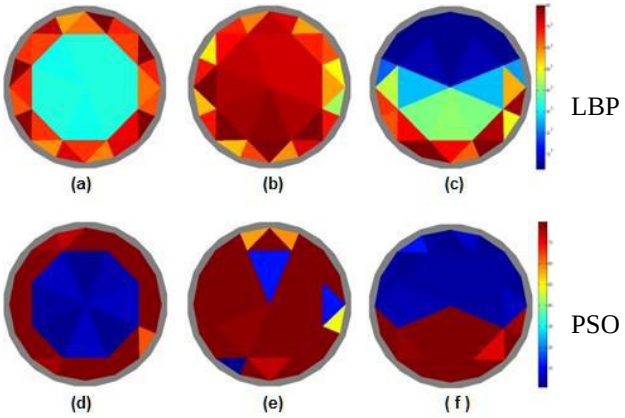

Figure 4. Reconstructed images from simulated values without numerical noise of 3%.

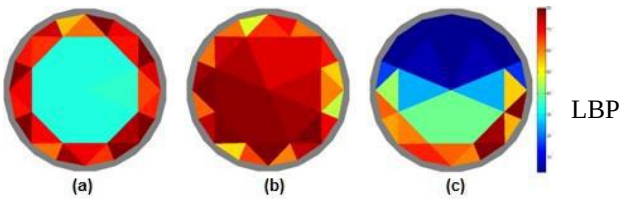

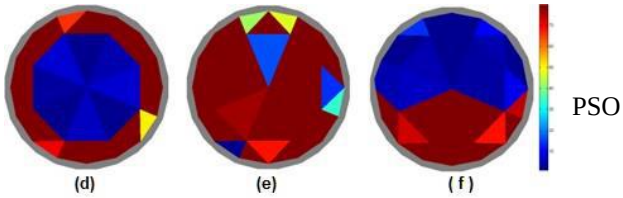

Fig.5. Reconstructed images from simulated values without numerical noise of 5%.

IV. DISCUSSION

PSO technique applied to ECT imaging has compelling results concerning its potentiality. Even in the presence of noise, it is possible to observe, not only visually but also by the quality indicators above, a good agreement between the proposed permittivity models and the accomplished results for the distinct flow patterns tested.

V. CONCLUSION

However, one of the main limitations of PSO technique is reached when the complexity of the optimization functional increases in conjunction with the amount of image pixels and, therefore, the number of parameters to be determined. This situation limits the maximum image resolution that can be achieved in real time applications. A possible solution is to grow the swarm size, which facilitates the determination of an optimal solution, but such approach is time consuming when a single processing unit is employed.

REFERENCES

[1] BELO, F.A. AND MOURA, L.F.M. (1999). *A high frequency electronic transducer for multiphase flow measurements*, Journal of the Brazilian Society of Mechanical Sciences, 21(4), 611-621.

[2] CUI, Z., YANG, C., SUN, B. AND WANG, X. (2014). *Liquid Film Thickness Estimation using Electrical Capacitance Tomography.* Measurement Science Review, 14(1), pp. 8-15.

[3] EBERHART, R.C. AND SHI, Y. (2001). *Particle swarm optimization: developments, applications and resources*, in Proceedings of the Congress on Evolutionary Computation 2001 (CEC '01), Seoul, Korea. Piscataway, NJ: IEEE Service Center, pp. 81-86.

[4] KENNEDY, J. AND EBERHART, R.C. (1995). *Particle swarm optimization.* Proc. IEEE Int'l. Conf. on Neural Networks, IV, Piscataway, NJ: IEEE Service Center. pp. 1942-1948.

[5] LI, KEZHI, (2015). *A Brief Survey of Image Processing Algorithms in Electrical Capacitance Tomography*, CoRR, arXiv preprint arXiv:1510.04585.

[6] MEI, I.L.S., ISMAIL, I., SHAFQUET, A. AND ABDULLAH, B. (2016). *Real-time monitoring and*

measurement of wax deposition in pipelines via non-invasive electrical capacitance tomography, Measurement Science and Technology, 27(2), pp. 25403-25413.

[7] SCHUTTE, J. F., REINBOLT, J. A., FREGLY, B. J., HAFTKA, R. T. AND GEORGE, A. D. (2004). *Parallel global optimization with the particle swarm algorithm*, International journal for numerical methods in engineering, 61(13), p. 2296.

[8] SHI, Y. AND EBERHART, R.C. (1998). *Parameter selection in particle swarm optimization*. In Evolutionary Programming VII: Proc. EP98, New York: Springer-Verlag, pp. 591-600.

[9] SINGH, N. (2012). *Parallel Astronomical Data Processing or How to Build a Beowulf Class Cluster for High Performance Computing?* Centre for Astronomy, School of Physics National University of Ireland, Galway.

[10] SMOLIK, W. T. (2010). *Accelerated Levenberg-Marquardt method with an optimal step length in electrical capacitance tomography*, International Conference on Imaging Systems and Techniques, IEEE, pp. 204-209.

[11] SOUZA, B. C. B. N. (2009). *Resolução do problema direto da técnica de reconstrução de imagens via tomografia capacitiva elétrica aplicada ao estudo de sistemas multifásicos*, Dissertação de Mestrado, UFPB, João Pessoa-PB.

[12] THORN, R., JOHANSEN, G. A. AND HJERTAKER, B. T. (2013). *Three-phase flow measurement in the petroleum industry*, Meas. Sci. Technol., vol. 24, no. 1, pp. 012003.

[13] WIRGIN, A (2004). *The inverse crime*, arXiv preprint math-ph/0401050.

[14] YANG, W.Q. AND PENG, L. (2003). *Image reconstruction algorithms for electrical capacitance tomography*, Meas. Sci. Tech. 14, 2003, pp. 1-13.

[15] ZAINAL-MOKHTAR, K. AND MOHAMAD-SALEH, J. (2013). *An Oil Fraction Neural Sensor Developed Using Electrical Capacitance Tomography Sensor Data*. Sensors 13, no. 9: pp. 11385-11406.